Chemical Engineering Journal 390 (2020) 124509

Contents lists available at ScienceDirect

Chemical Engineering Journal

journal homepage: www.elsevier.com/locate/cej

Process analysis overview of ionic liquids on CO_2 chemical capture

D. Hospital-Benito, J. Lemus, C. Moya, R. Santiago, J. Palomar*

Chemical Engineering Department, Universidad Autónoma de Madrid, 28049 Madrid, Spain

HIGHLIGHTS

- Different ILs are evaluated as CO_2 chemical absorbents by process analysis.
- CO_2 solubility, viscosity and heat of reaction are stated as key IL properties.
- Major exothermic reactions overcome kinetic limitations at adiabatic conditions.
- Reaction enthalpy determines solvent requirement, energy demand and column sizes.

GRAPHICAL ABSTRACT

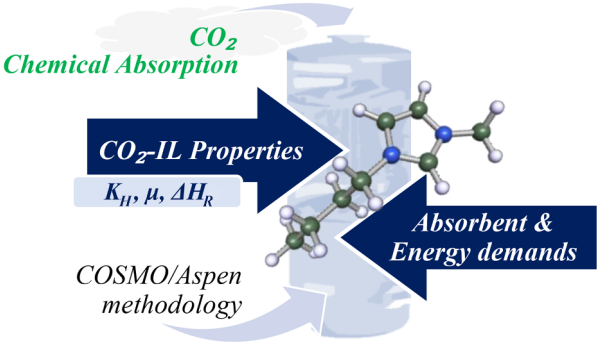

ARTICLE INFO

Keywords:
CO_2 capture
Ionic liquids
Chemical absorption
Process simulation
COSMO-based/Aspen

ABSTRACT

A process analysis overview of the ionic liquids (ILs) performance as chemical absorbents in post-combustion, biogas and pre-combustion CO_2 capture systems was carried out. Six representative ILs, among them carboxylate, aminoacid and aprotic heterocyclic anion-based ILs -with remarkably different CO_2 absorption thermodynamics and kinetics- were selected. COSMO-based/Aspen Plus methodology, supported with available experimental data, was successfully applied to design the absorption and regeneration stages in commercial packed columns to reach a 90% CO_2 recovery at different CO_2 partial pressures and given operating conditions, for comparison purposes. The IL performance in CO_2 capture process was evaluated by means of solvent need, energy consume and column size. The CO_2-IL reaction enthalpy and IL viscosity were identified as key properties to guide solvent selection. For the considered ILs, increasing the reaction exothermicity means lower solvent, energy and equipment requirements as liquid viscosity descends, overcoming mass transfer limitations at adiabatic conditions. The CO_2 capture process efficiency was successfully related to the thermodynamic gap capacity given by CO_2-IL isotherms at the absorption/regeneration operating conditions. AHA-IL family is aimed as a promising alternative to industrial CO_2 chemical absorbent benchmark (aqueous amine solution) due to their advantageous key properties: moderate viscosity and adequate compromise between high CO_2 solubility and reaction enthalpy. Current results indicated the technical viability of ILs-based CO_2 capture processes compared to available technologies, but further analysis (*i.e* cost estimations, environmental impacts and life cycle assessment) are required to ensure the sustainability of a new process.

* Corresponding author.
E-mail address: pepe.palomar@uam.es (J. Palomar).

https://doi.org/10.1016/j.cej.2020.124509
Received 22 December 2019; Received in revised form 17 February 2020; Accepted 18 February 2020
Available online 19 February 2020

1. Introduction

Carbon dioxide (CO_2) capture and storage (CCS) is a demanding technology for the decarbonization of our global economy. Fossil fuel power plants are still the major source of this main greenhouse gas [1,2]. Solvent-based CO_2 capture through both physical and chemical absorption has been widely studied and proposed as an available technique [3]. Regarding physical absorption, organic solvents such as Selexol are currently applied in industrial processes like natural gas purification or Integrated Gasification Combines Cycle power plants as a pre-combustion capture technique. These processes work at high operating pressures, showing elevated electric power consumption [3–5]. Amine-based processes are the most established and economically viable chemical absorption technology for carbon capture nowadays [6–8]. This technique is more versatile, being employed at both low and high CO_2 partial pressures [5]. Monoethanolamine (MEA) aqueous solution (30 wt%) is the most common solvent used for post-combustion flue gas treatments [9,10] or biogas upgrading [11] due to its high absorption capacity at low CO_2 partial pressure and low viscosity [12]. However, relevant drawbacks such as an energy intensive regeneration unit for the desorption of CO_2 (-85 kJ/mol exothermic reaction), great solvent loss, degradability and corrosiveness [13,14] promote the research of alternative solvents with better properties to address these deficiencies.

In this sense, ionic liquids (ILs) are being investigated as potential CO_2 absorbents since they present favorable properties for CO_2 capture like high uptake capacity, negligible vapor pressure, wide liquid temperature range and tunable solvent capacity [15–19]. First, ILs presenting CO_2 physical absorption were initially put forward as suitable solvents. Their CO_2 solubility was enhanced by the appropriate choice of the anion and cation forming the IL. Rising the cation alkyl side chain and fluorinating the anion improved the molar solubility [20] but, it was demonstrated that the mass CO_2 solubility was not especially higher than conventional organic solvents in ILs with high-ranking molar weights [21]. Furthermore, it was recently reported that CO_2 uptake is also determined by the transport properties when realistic operating conditions are considered in packing columns, hence CO_2 physical absorption using ILs is strongly kinetically controlled owing to their huge viscosity [22–24]. To overcome the mass transfer limitations, different strategies have been followed: i) enhancing the CO_2 diffusivity by proposing ILs based on anions like dicyanamide $[DCN]^-$ or tricyanomethanide $[TCM]^-$ resulting in relatively low viscosity besides good mass solubility [23,25,26]; and ii) increasing the gas–liquid contact surface by supporting [27] or encapsulating [24,28] the IL solvent.

Alternatively, ILs were functionalized to chemically react with CO_2, upgrading the absorption capacity [16,29–32]. It is possible to improve the absorption capacity modifying the structure of the IL, leading to an increase of the stoichiometry and reaction enthalpy or reducing the CO_2-IL mixture viscosity. Consequently, some IL families can be found depending on the selected functional group [18]. Carboxylate-based imidazolium ILs may be considered the pioneers and most widely studied ILs for CO_2 chemical absorption [33–35]. Particularly, [Bmim][acetate] is a reference solvent when using ILs as CO_2 chemical absorbents [36,37]. It has been demonstrated that the reaction follows a 1:2 stoichiometry by both experimental and computational works, showing that CO_2 reacts with the cation to form a carboxylate [36,38]. Acetate-based ILs heats of reaction were measured resulting in almost -39 kJ/mol [39], significantly lower exothermirticity than that found for the benchmark MEA reactant (-85 kJ/mol [12]). The available publications warn in regards to their thermal stability reporting relevant weight loss above 373 K at isothermal TGA runs for [Bmim][acetate] [40]. Moreover, strongly unfavorable mass transport properties of this IL and its reaction product were found, mainly because of their high viscosity [41,42]. Additional troubles were discovered when regenerating this IL, suggesting an irreversible reaction between CO_2 and [Bmim][acetate] [38,43]. Encapsulated or supported ILs [44,45], or co-solvent mixing [46] has been proposed to get over the mass transfer kinetic control. Recently, ILs derived from safe amino acid anions (aa-ILs), particularly hopeful from a eco-friendly and sustainable point of view due to their non-toxic biodegradability and plenty availability have also been reported as good CO_2 chemical absorbents attending to thermodynamics [47–49]. Although the exact reaction mechanism of CO_2 in aa-ILs is still under discussion, the zwitterion type mechanism with a 1:2 stoichiometry of reaction has been commonly proposed [50]. These ILs present moderate enthalpy of reaction (from –16 to -35 kJ/mol) and thermal stability [50] but huge viscosity values (specially while reacting with CO_2), needing to be supported or encapsulated to solve their kinetic limitations in CO_2 capture [48,50]. On the other hand, ILs with aprotic heterocyclic anions (AHA-ILs), chiefly those based on the 2-cyanopyrrole anion ([CNPyr]), are promising candidates for CO_2 chemical absorption because of their high solubility even at low CO_2 partial pressures, high thermal and chemical stability and high reaction rates [51–55]. Their advantageous 1:1 stoichiometry chemical reaction consists in the CO_2 bonding with the anion by reversible carboxylation without a significant increase in viscosity [19]. The reaction enthalpy of these ILs with CO_2 (from -37 to -54 kJ/mol) is also tunable and they present high decomposition temperatures [52]. Nevertheless, AHA-ILs viscosity is relatively low compared to other ILs used as CO_2 chemical absorbents (around 100 mPa·s at 323 K for [CNPyr]-based AHA-ILs), but still high respect to aqueous amine solutions or organic industrial CO_2 absorbents [53]. Supporting or encapsulating AHA-ILs [56] as well as using co-solvents, such as tetraglyme [57,58], are alternatives to overcome these transport limitations.

In order to evaluate the CO_2 absorbent performance at industrial scale, lots of researching efforts have been driven towards the description of solvent-based CO_2 capture processes using process simulation. Several publications studied CO_2 physical absorption with organic solvents [4,5], CO_2 chemical absorption using amine-based systems [9,10,13] or aqueous ammonia [59], some of them performing detailed energetic and economic analyses and considering mass transfer in the simulation through rigorous Rate-based calculation. Recently, some papers have emphasized the need of addressing the challenges associated with thermophysical and transport properties of common CO_2 absorbents because of their significant contribution over process performance and cost [12,60]. Regarding CO_2 capture processes based on absorption with ILs, process simulation was used to carry out thermodynamic, kinetic and process analyses using ILs that present CO_2 physical absorption, evaluating solvent and energy requirements, performing cost estimation and comparing to amine aqueous solutions [14,22,60–63]. The resulting mass flows of IL needed were found higher than other technologies but showing lower energy demand. ILs that chemically absorb CO_2 have been also studied using process simulation. The post-combustion CO_2 capture process based on [Bmim][acetate] was modeled taking into account only the thermodynamic behavior, reporting lower energy needs (3.2 GJ/t_{CO2}) and investment costs than MEA [64]. The $[P_{66614}][CNPyr]$, an aprotic hetero-cyclic anion (AHA)-based IL, performance for post-combustion CO_2 capture was also evaluated through process simulation, determining an energy for IL regeneration of 3.6 GJ/t_{CO2} [65]. Taking into account the kinetics in the process, mixtures of tetraglyme and AHA-ILs has been proposed to improve the CO_2 absorbent performance in packed columns, descending the energy demand to 1.4 GJ/t_{CO2} [57].

This work aims to identify key properties that govern the IL performance in CO_2 capture processes by chemical absorption, with the purpose of establishing reliable IL selection criteria. To ensure that, an Aspen Plus supported evaluation of 6 representative IL chemical absorbents in three different CO_2 capture process configurations (post-combustion, pre-combustion and biogas upgrading) was carried out and compared at given operating conditions. The ILs analyzed were triethyloctylphosphonium 2-cyanopyrrole ($[P_{2228}][CNPyr]$), trihexyltetradecylphosphonium 2-cyanopyrrole ($[P_{66614}][CNPyr]$), 1-butyl-3-

methylimidazolium acetate ([Bmim][acetate]), 1-butyl-3-methylimidazolium isobutyrate ([Bmim][i-but]), 1-butyl-3-methylimidazolium glycinate ([Bmim][GLY]) and 1-butyl-3-methylimidazolium prolinate ([Bmim][PRO]) (Table S1). A multiscale COSMO-based/Aspen Plus methodology is applied to perform the detailed assessment [66]. For this purpose, thermodynamic and kinetic models were fitted to experimental data at different temperatures in order to determine the parameters required to describe both the physical and chemical CO_2 absorption in IL (viscosity, reaction enthalpy, equilibrium and Henry's constants) using Aspen Plus software. RADFRAC packed columns on Rate-based mode were used to design the individual absorption and regeneration (stripping) operations to achieve a 90% of CO_2 recovery with the 6 different ILs. Finally, the stripping column was interconnected to the absorption operation with the purpose of analyzing the recirculation effect on the complete CO_2 capture process for the best three ILs. Solvent need, regeneration energy duty and column size were analyzed as the main metrics for reviewing the CO_2 capture performance of the ILs, focusing on detecting absorbent properties impacts on the overall CO_2 capture process for post-combustion, biogas and pre-combustion systems. The obtained results were conveniently compared to other available technologies in order to revise the viability of using ILs as alternative CO_2 chemical absorbents.

2. Computational details

2.1. Component definition and property method

CO_2 capture process was modeled employing Aspen Plus v10 commercial process simulator using three different process configurations: post-combustion, biogas and pre-combustion in order to analyze CO_2 partial pressure and gas flow effects with representative industrial cases. The six ILs and their reaction products were added as pseudo-components into the simulator following a multiscale COSMO-based/Aspen Plus methodology previously reported by our group [46,57,66]. The complete procedure employed to include new non-databank compounds into Aspen Properties and to generate simulations entailing them was described in detail in prior works of our group [66]. As summary, quantum chemical structure optimizations and COSMO-RS calculations of the ILs and their reaction products were carried out to fully specify the COSMOSAC property method. COSMOSAC in code 1 was selected to carry out the simulations [66]. To allow better description of the CO_2 mass transfer process, the experimental temperature dependent ILs viscosity data is included into the Aspen Properties in the form of Andrade equation (Eq. (1)).

$$Ln\mu_i = A_i + \frac{B_i}{T} \tag{1}$$

To describe the chemical absorption of CO_2 in the selected ILs using Aspen environment, the ILs experimental isotherms performed by gravimetric measurements were adjusted to a thermodynamic model in which the physical absorption is described by Henry's Law (Eq. (2)) and the chemical equilibrium reaction by Eqs. (3) and (4) depending on the stoichiometry:

$$x_{CO_2} = \frac{P_{CO_2}}{K_H} \tag{2}$$

$$K_{eq} = \frac{x_{PROD}}{x_{IL}\cdot x_{CO_2}} \tag{3}$$

$$K_{eq} = \frac{x_{PROD}}{x_{IL}^2\cdot x_{CO_2}} \tag{4}$$

A combination of these equations leads to Eqs. (5) and (6) that describe both CO_2 physical (first term) and chemical (second term) absorption according to the right stoichiometry of reaction with CO_2 depending on the IL.

AHA-ILs 1:1 stoichiometry ($IL + CO_2 \rightleftharpoons PROD$):

$$z = \frac{P_{CO_2}}{K_H - P_{CO_2}} + \frac{K_{eq}\cdot P_{CO_2}\cdot C}{K_H + K_{eq}\cdot P_{CO_2}} \tag{5}$$

Carboxylate based ILs and aa-ILs 1:2 stoichiometry ($2IL + CO_2 \rightleftharpoons PROD$):

$$z = \frac{P_{CO_2}}{K_H - P_{CO_2}} + \frac{-2\cdot K_{eq}\cdot\frac{P_{CO_2}}{K_H} + \sqrt{K_{eq}\cdot\frac{P_{CO_2}}{K_H}}}{1 - 4\cdot K_{eq}\cdot\frac{P_{CO_2}}{K_H}} \tag{6}$$

where z is the molar ratio of CO_2 absorbed per mol of IL, P_{CO2} is the CO_2 partial pressure in bar, K_H is the CO_2 Henry's law constant in the IL in bar, K_{eq} is the reaction equilibrium constant and C is the ratio of AHA-IL available to react with CO_2 molecule and the total AHA-IL as reported in previous literature [52]. In this work, $C = 0.92$ for $[P_{2228}][CNPyr]$ and 0.89 for $[P_{66614}][CNPyr]$ is used.

The equilibrium constant of Eq. (7) was incorporated into Aspen Plus Reactive-Distillation equilibrium reaction and it was used to determine the parameters needed by Aspen Plus to perform the reactions between CO_2 and each IL. Therefore, Aspen Plus estimates the right equilibrium constant value that fits the isotherm equation (Eqs. (5) or (6)) at different temperatures.

$$LnK_{eq_i} = A_i + \frac{B_i}{T} \tag{7}$$

The enthalpy of reaction (expressed per mole of reacted CO_2) is obtained as the product of the estimated parameter B_i of Eq. (7) multiplied by the ideal gas constant (8.314 J/mol·K), which was translated into IL enthalpy of formation using the equilibrium reactor model, so as to be introduced into Aspen Properties.

CO_2 was defined as Henry component into Aspen Properties. Aspen Plus Henry's component definition requires the temperature dependence of the parameter (Eq. (8)), used to estimate the ILs Henry's constants that suit the experimental isotherms.

$$LnK_{H_i} = A_i + \frac{B_i}{T} \tag{8}$$

Henry's constant value cannot be introduced directly as calculated in the Aspen Plus software as it considers the CO_2 activity coefficient (γ_{CO_2}) in the simulator definition: $x_{CO_2} = \frac{P_{CO_2}}{K_H\cdot\gamma_{CO_2}}$, so it needs a correction to Henry's constant value. An iterative procedure was used to adjust Aspen Henry's constant (K_H') to experimental physical solubilities predicted by the isotherms (Eqs. (5) and (6)). All thermodynamic and kinetic parameters used to define the CO_2-IL systems in Aspen Plus software are collected in Table S2 of Supplementary Material.

2.2. Stream models and complete processes design

This work comprises post-combustion and pre-combustion gas treatment as well as biogas upgrading operating conditions. The characteristic inlet gas stream for each case was specified according to the data summarized in Table 1. Compositions are simplified to two major constituents (CO_2 plus a priori inert gas: N_2, H_2 or CH_4), so other typical compounds such water or sulfur dioxide are not included in this study.

Table 1
Feed gas streams properties.

		Post-combustion	Biogas	Pre-combustion
Inlet temperature (K)		313	313	313
Total pressure (MPa)		0.10	0.32	3.27
CO_2 partial pressure (MPa)		0.01	0.12	1.31
CO_2 molar flow (kmol/h)		100	100	100
Composition	x_{CO_2}	0.13	0.38	0.40
	x_{N_2}	0.87	–	–
	x_{CH_4}	–	0.62	–
	x_{H_2}	–	–	0.60

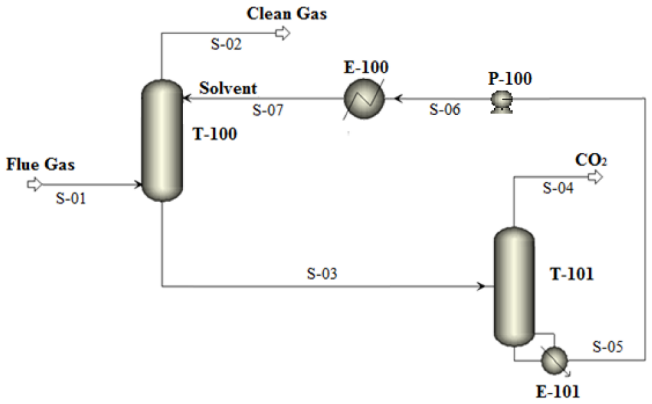

Fig. 1. Complete ILs-based process diagram proposed for CO_2 chemical absorption.

The conceptual engineering of the ILs-based process proposed for CO_2 capture through chemical absorption is shown in Fig. 1. The gas stream to be treated (S-01) is fed to the absorption column (T-100) at the inlet conditions summed up in Table 1 where contacts the recirculated IL from the regeneration stripping column (S-07) at adiabatic operating conditions. After absorbing a 90% of the CO_2 fed, the treated gas stream (S-02) exits the absorber through its head. The regeneration unit (T-101) receives the saturated absorbent stream (S-03). In this configuration, there is not preheating step, so the column reboiler (E-101) supplies the heating required to achieve the IL regeneration in which the obtained IL purity is around 90 wt% in all cases. The CO_2 captured leaves the column after its desorption (S-04) and the IL regenerated (S-05) is pressurized (P-100), cooled (E-100) and recirculated to the absorption column (S-07).

2.3. CO_2 absorption column

CO_2 absorption column (T-100 in Fig. 1) was modeled as a packed column using RADFRAC rigorous model implemented as default in Aspen Plus v10, considering adiabatic operating conditions and performing the calculations in Rate-based mode with the reaction module enabled. The chemical reaction between each IL and CO_2 was specified using the Reactive-Distillation equilibrium reaction equation included by default in Aspen Plus to specify reactions to be used with RADFRAC column model. The K_{eq} equation (Eq. (7)) is specified with parameters A_i and B_i that were estimated from the experimental isotherms as explained before. The liquid is the reaction phase for all cases and the equilibrium constant basis is the mole fraction.

The gas was fed with a constant flow of 100 kmol/h of CO_2 at 313 K and CO_2 partial pressures from 0.013 to 1.3 MPa in order to study its influence in the CO_2 capture, thus the absorber operates at inlet stream total pressure. The three different inlet gas stream models for pre-combustion, biogas and post-combustion CO_2 capture are grouped in Table 1. The column is 15 m of height, discretized by 10 stages, and with a variable diameter able to keep a fractional capacity of 80% in all the simulations. The Flexipac 700Y structured packing was selected in the absorber. The required IL mass flow to achieve a 90% of CO_2 uptake rate, the IL conversion and column diameter were calculated for each system.

2.4. ILs regeneration column

The column T-101 of the process diagram (Fig. 1) is the absorbent regeneration unit. It consists in a stripping column in which the reboiler supports the sensible heat to achieve the regeneration temperature, the energy needed to generate the vapor stripping stream (mainly the CO_2 desorbed) and the energy required to turn back the chemical reaction between CO_2 and each IL. A temperature of 373 K and 0.01 MPa of vacuum pressure are fixed as regeneration conditions in order to avoid IL thermal decomposition [40]. The vacuum energy was estimated by Aspen Plus compressor model emulating the pressure drop from 0.1 to 0.01 MPa directly to the vapor. The liquid stream (S-03) that leaves the absorber (T-100) is the inlet stream of this regeneration column (T-101) without carrying out any preheating that involves energy saving. The RADFRAC model operating in Rate-Based mode -including the same Reactive-Distillation reaction, equal height (15 m) and type (Flexipac 700Y) of packing and 6 calculation stages- was utilized to simulate the stripping column. The regeneration energy required and column diameter for a fractional capacity of 80% were determined in each case.

2.5. Complete process

Once both absorption and desorption operations were evaluated at open cycle, IL recirculation was closed as depicted in Fig. 1 for the best three ILs to study the effect of the partial regeneration in the process performance. Secondary blocks for conditioning (E-100 and P-100) the solvent stream that enters the absorber (S-07) were added on, although their energy demands are not taken into account in this work. In this section, the influence of recirculating the absorbent is analyzed. Gap capacity variable is introduced to discuss the complete process results and differentiated in 2 types: i) Process gap capacity describes the difference between rich (S-03) and lean absorbent (S-07) loading capacity, which represents the real absorbent capacity in the complete process (considering the solvent regeneration), hence it is particularly useful to explain the absorbent demand and ii) Thermodynamic gap capacity that define the same difference but calculated through the ILs isotherms at 313 K (absorber inlet conditions) and 373 K (reboiler temperature) at the corresponding CO_2 partial pressure.

3. Results

3.1. Absorption properties

The physical and chemical properties of the 6 studied CO_2-IL systems estimated by current approach in Aspen Plus are collected in Table 2. The considered ILs present a relatively wide range of molar weight (200–600 g/mol), being $[P_{66614}][CNPyr]$ the heaviest IL, whereas [Bmim][acetate] is the lightest. On the other side, all ILs present similar density but remarkably different viscosity. AHA-ILs are the lowest viscous (163–166 mPa·s) whereas aa-ILs have significant high viscosity values (424–891 mPa·s) and caboxylate-based ILs present intermediate values, but all of them two magnitude orders ahead of

Table 2
Estimated physical properties, Henry's (K_H) and reaction equilibrium (K_{eq}) constants and enthalpy of reaction (ΔH_R), of selected ILs at 313 K, using Aspen Plus.

	MW (g/mol)	ρ (kg/m^3)	μ (mPa·s)	K_H (MPa)	K_{eq}	ΔH_R (kJ/mol)
$[P_{2228}][CNPyr]$	322.47	940	163.45	6.70	1389.84	−47.72
$[P_{66614}][CNPyr]$	574.95	900	166.42	3.93	421.61	−39.77
[Bmim][acetate]	198.26	1030	179.79	9.31	65.56	−35.12
[Bmim][i-but]	226.32	1010	198.02	13.57	25.40	−19.38
[Bmim][GLY]	213.28	1030	423.87	18.06	6.78	−22.92
[Bmim][PRO]	253.34	1060	891.32	17.15	5.60	−14.03

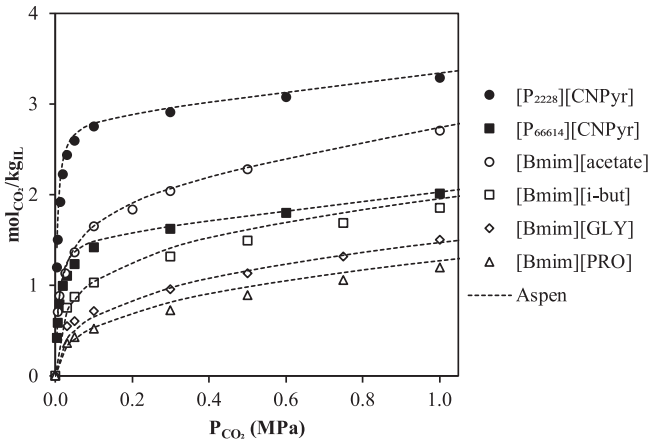

Fig. 2. Experimental (symbols) *vs.* calculated (lines) CO_2 absorption isotherms of 6 ILs at near 313 K.

current amine-based solutions [12] or organic physical solvents like tetraglyme [32] (1–3 mPa·s).

The avaliable experimental isotherms are successful fitted to the proposed thermodynamic models (Eqs. (5) and (6)). For comparison purposes, Fig. 2 and Table 2 show the results at 313 K. The CO_2 physical absorption capacity of ILs can be compared according to Henry's constant. The lowest K_H values -what mean advantageous physical solubility- were found for AHA-ILs, especially for [P_{66614}][CNPyr] (3.9 MPa) which own similar K_H to industrial physical CO_2 absorbents such as tetraglyme [32]; in contrast, aa-IL presents comparatively high Henry's constants (K_H > 17 MPa), whereas caboxylate-based ILs present intermediate CO_2 physical absorption capacity. The chemical CO_2 absorption is related to the obtained reaction equilibrium constant (K_{eq}) and heat of reaction (ΔH_R) in Table 2, which are in good agreement with experimental values reported in previous publications for [P_{66614}][CNPyr] (4.7 MPa and −43 kJ/mol at 313 K) [56], [Bmim][acetate] (−39 kJ/mol) [39], [Bmim][GLY] (19.5 MPa and −19 kJ/mol at 318 K) and [Bmim][PRO] (18.6 MPa and −16 kJ/mol at 318 K) [50].

As can be seen, AHA-ILs also present a favored chemical reaction with CO_2 in comparison to carboxylate anion-based ILs and aa-ILs, because of their higher K_{eq} (reaction more displaced to products) and more negative ΔH_R values (more exothermic reaction). Anyhow, the reversibility of all CO_2-IL reactions is more favorable compared to MEA (−85 kJ/mol at 313 K) [12,52].

The calculated thermodynamic and thermochemical properties previously presented allow the simulation of CO_2 absorption phenomena in ILs by Aspen Plus. The equilibrium isotherms estimated by the process simulator were compared to the experimental CO_2 solubility data so as to validate our multiscale methodology. Fig. 2 represent the experimental and calculated CO_2-IL isotherms at 313 K (inlet absorption temperature) for the studied six ILs.

As can be seen in Fig. 2, the 6 CO_2 isotherms at 313 K are properly represented by Aspen calculations (R^2 > 0.99) (see also Figs. S1 and S2 in Supplementary Material for other temperatures) and also illustrates that chemical absorption dominates at low CO_2 partial pressures and how physical absorption takes place at high pressure (P > ~0.2 MPa). [P_{2228}][CNPyr] is the best overall absorbent when attending to thermodynamics, particularly at low pressure. The trend of CO_2 absorption capacity per mass of IL is as follow, [P_{2228}][CNPyr] > [Bmim][acetate] > [P_{66614}][CNPyr] > [Bmim][i-but] > [Bmim][GLY] > [Bmim][PRO], and it can be related to both favorable physical and chemical absorption (low K_H and high K_{eq}, respectively) and low molar weight (Table 2).

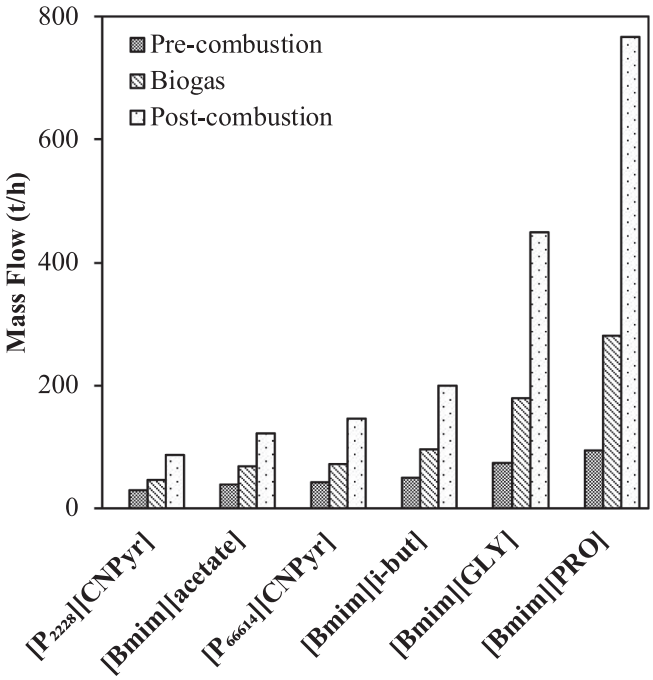

Fig. 3. IL requirement to achieve 90% of CO_2 capture rate at post-combustion, biogas and pre-combustion configurations (Table 1) and adiabatic conditions.

3.2. CO_2 absorption column

The RADFRAC column implemented in Aspen Plus was used to simulate the absorption operation at CO_2 partial pressures of 0.013 (post-combustion), 0.12 (biogas) and 1.3 MPa (pre-combustion) and adiabatic conditions. IL needs to achieve a 90% of CO_2 capture is analyzed. Fig. 3 shows the amount of absorbent required depending on the IL and CO_2 partial pressure.

As can be seen in Fig. 3, IL requirement in the absorption column is strongly determined by the inlet CO_2 partial pressure, drastically decreasing from post-combustion to biogas and to pre-combustion system. Comparing by absorbent, AHA-ILs are those with less consumes (the best case is [P_{2228}][CNPyr], 30–87 t/h), aa-ILs have the highest mass flow demand (74–767 t/h) and carboxylate-based IL present intermediate behavior.

In order to state the key properties of CO_2-IL systems that determines absorbent performance, Fig. 4 show the estimated viscosity and CO_2 solubility at absorber inlet conditions (313 K and CO_2 partial pressures from 0.013 to 1.3 MPa). It is clearly observed that ILs that present higher CO_2 solubility reduce the solvent demand. In addition, Fig. 4 also illustrates how the IL flow rate descends by increasing the pressure, since CO_2 solubility is improved. Thus, pre-combustion operating conditions are the most favorable for CO_2 capture. In fact, the minimum solvent demand (30 t/h) is obtained for [P_{2228}][CNPyr] at pre-combustion CO_2 partial pressure (40% lower than [Bmim][acetate] at the same conditions). Moreover, the role of viscosity is highlighted in the case of aa-ILs. Despite having solubilities only slightly lower than [Bmim][i-but], they do need higher mass flow rates to meet the required purity. Thereby, evident mass transfer limitations are found for these ILs due to their viscosity as it was demonstrated in previous publications [50].

Fig. 5 shows the viscosity dependence with the temperature of absorber outlet liquid (S-03 stream in Fig. 1). Since the absorption column works at adiabatic conditions, the IL is being heated because of the heat of reaction. A synergistic effect between thermodynamics and kinetics is observed for the studied ILs. IL with higher CO_2 absorption capacity (lower IL flow requirement) implies a higher outlet temperature, up to 368 K for [P_{2228}][CNPyr], which reduces its viscosity, consequently

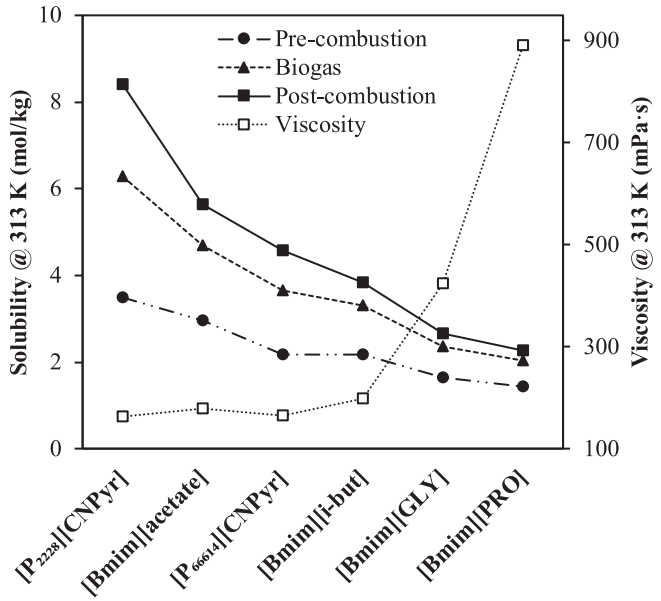

Fig. 4. CO_2 solubility in IL along with IL viscosity (S-07 stream) at 313 K and post-combustion, biogas and pre-combustion pressures (Table 1).

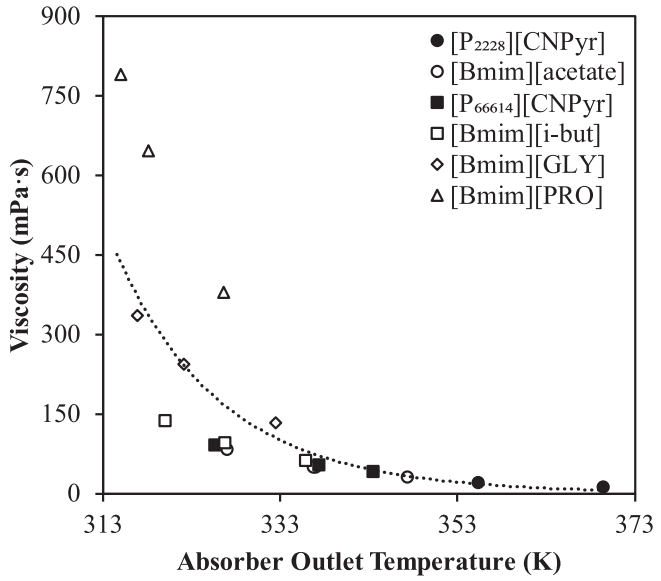

Fig. 5. ILs viscosity at absorber outlet liquid flow (S-03) temperature.

improving the mass transfer rates and reducing further the solvent requirements, effect that magnifies at higher partial pressures. Although an increase of the outlet temperature reduces the solubility of CO_2 in IL, the increase in mass transfer compensates this effect improving the efficiency of the global process. In the case of aa-ILs, viscosity is not reduced enough (133 – 790 mPa·s) to avoid the kinetic control as it does for [P_{2228}][CNPyr] (49–12 mPa·s) due to its hottest outlet temperature (more exothermic reaction) [57]. Therefore, the viscosity and the CO_2 solubility can be interpreted as two IL key properties to predict the absorption performance and then solvent requirements.

The grade of utilization of IL reactant is evaluated in terms of conversion. The IL conversion in the reaction with CO_2 at the proposed operating conditions as well as their equilibrium constants (Table 2) are presented in Fig. 6.

As expected, the IL conversion increases with CO_2 partial pressure, because the bigger CO_2 concentration favors the reaction toward products. At the same time, the ILs with highest IL conversion are those with the greatest reaction equilibrium constants. Two different slopes

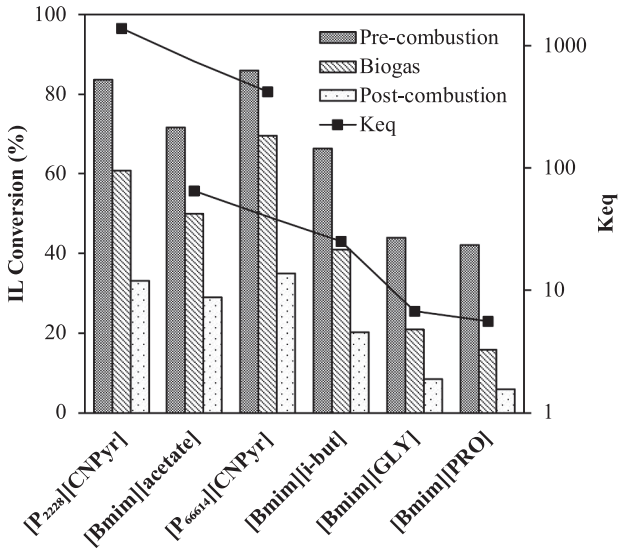

Fig. 6. IL conversion in the absorber and K_{eq} values for CO_2 + IL reaction at 313 K and post-combustion, biogas and pre-combustion pressures.

(dots in Fig. 6) are marked in regards on whether the stoichiometry of reaction is 1:1 or 2:1. AHA-ILs (1:1 stoichiometry), give the best conversions overall, so it means that 1:1 stoichiometry is the most favorable for an efficient use. Although [P_{66614}][CNPyr] presents lower equilibrium constant (421.6) than [P_{2228}][CNPyr] (1389.8), it reaches little upper conversion because at adiabatic conditions [P_{2228}][CNPyr] suffers major heating, what slightly decreases the K_{eq} value. [P_{66614}][CNPyr] is the IL that achieves the best conversion values that goes from a 35% for post-combustion CO_2 capture to a 86% for pre-combustion followed from behind by [P_{2228}][CNPyr] with 33% and 84%, respectively. [Bmim][acetate] is the IL with 2:1 stoichiometry having superior K_{eq} (65.6) besides better conversion (29–72%) and [Bmim][PRO] is the worst one (K_{eq} = 5.6 and conversion from 6 to 42%).

Fig. 7 illustrates the relationship between the equilibrium constant (K_{eq}) and the reaction enthalpy (ΔH_R) for the 6 CO_2-IL systems at 313 K. ILs with higher K_{eq} and conversion values (AHA-ILs and [Bmim][acetate]) exhibit more exothermic reactions (from −35 to −48 kJ/mol). Thus, obtained equilibrium constants are directly governed by the

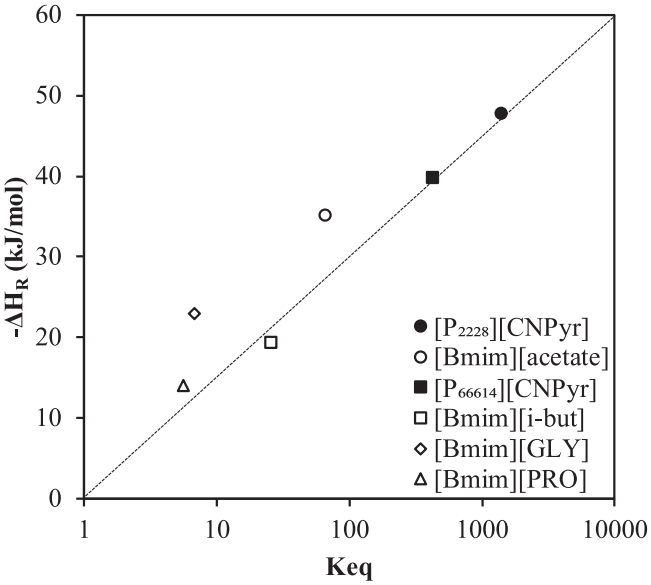

Fig. 7. Comparison of reaction enthalpy ($-\Delta H_R$) *vs.* equilibrium constant (K_{eq}) for the studied CO_2 + IL systems at 313 K.

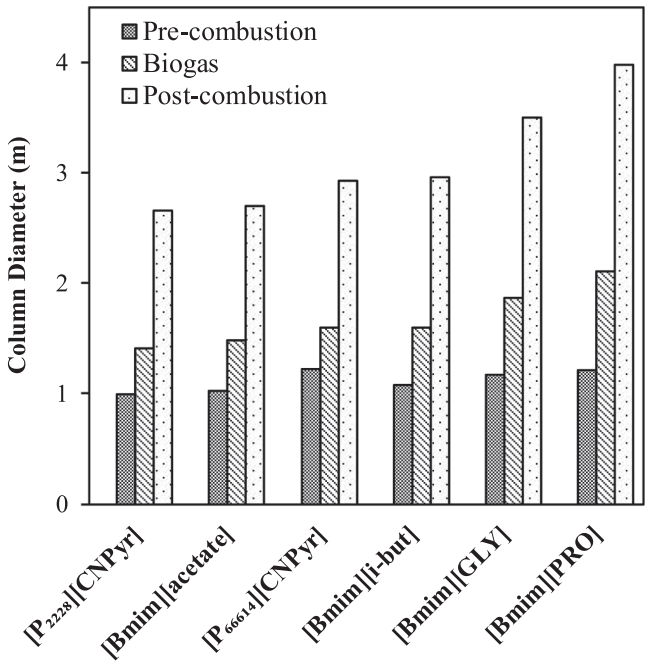

Fig. 8. Absorption column diameter depending on the IL and the process configuration.

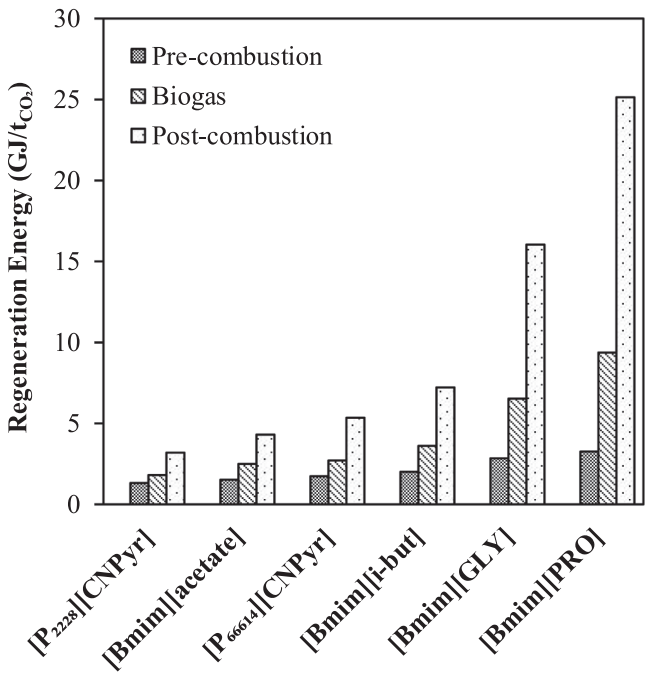

Fig. 9. Regeneration energy needs for each IL depending on the absorption process configuration.

enthalpic contribution to CO_2 chemical absorption in these ILs. Thereby, AHA-ILs are placed as the IL-family that present the greatest K_{eq} and hence clearly higher conversions owing to their raised enthalpies of reaction (around −40 kJ/mol, see Table 2). Current results indicate that the heat of reaction can be considered a key property to predict the IL utilization in the absorber unit as the heating effect at adiabatic conditions greatly improves the efficiency of the operation.

After analyzing the IL performance regarding solvent demand and conversion, preliminary column sizing was carried out. Fig. 8 reports the absorption column diameter calculated for each IL at the three different operating conditions.

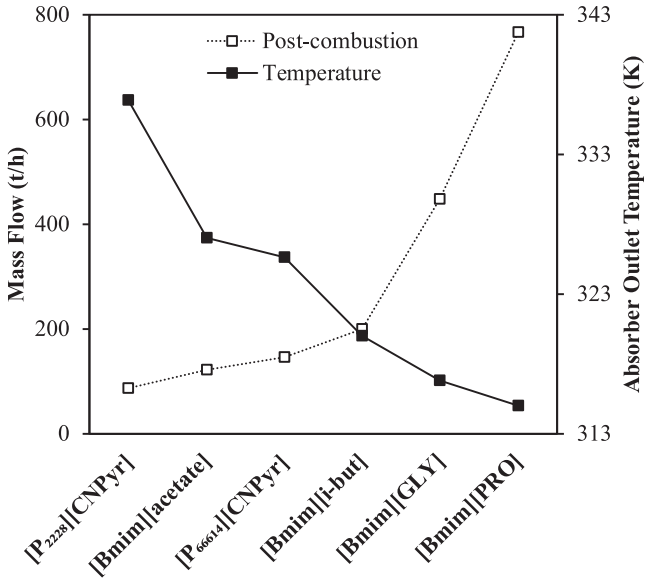

Fig. 10. Temperature and mass flow of the CO2-IL saturated stream (S-03) fed to regeneration column for post-combustion CO_2 capture.

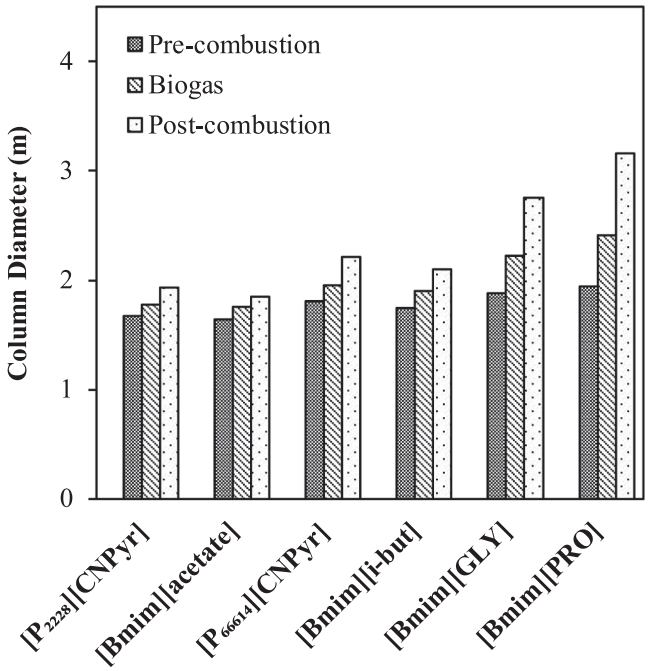

Fig. 11. Stripping column diameter depending on the IL and the process configuration.

Fig. 8 shows the same trend than the required amount of IL (Fig. 3). Thereby, [P_{2228}][CNPyr] needs smaller column diameters (from 1 m for pre-combustion to 2.7 m for post-combustion capture) than the worse aa-ILs (with values between 1.2 and 4 m). Likewise, post-combustion gas flow is moderately higher than in the other cases, contributing to bigger column sizes. Designed columns (15 m high) present industrial-range length to diameter ratios (5–30) [67], with the exception of those for aa-ILs at post-combustion CO_2 capture.

3.3. ILs regeneration column

The following part of the study disscusses the simulation results of IL regeneration stage. The regeneration column (T-101 in Fig. 1) was

Table 3
Complete process and individual operation results for CO_2 capture using $[P_{2228}][CNPyr]$, $[P_{66614}][CNPyr]$ and [Bmim][acetate] absorbents.

		Post-combustion		Biogas		Pre-combustion	
		Individual columns	Closed process	Individual columns	Closed process	Individual columns	Closed process
$[P_{2228}][CNPyr]$	S-07 IL mass flow (t/h)	87.0	96.9	46.7	49.9	29.8	31.5
	S-07 IL mass purity (%)	100.0	93.4	100.0	93.4	100.0	93.4
	IL conversion (%)	33.2	30.1	60.8	57.5	83.7	78.9
	Regeneration energy (GJ/tCO_2)	3.2	3.8	1.9	2.1	1.3	1.5
	Absorber diameter (m)	2.7	2.7	1.4	1.4	1.0	1.0
	Stripping diameter (m)	1.9	2.1	1.8	1.8	1.7	1.7
$[P_{66614}][CNPyr]$	S-07 IL mass flow (t/h)	146.8	167.6	71.8	76.2	43.4	45.0
	S-07 IL mass purity (%)	100.0	94.8	100.0	94.8	100.0	94.8
	IL conversion (%)	35.0	30.9	69.5	65.6	85.8	81.2
	Regeneration energy (GJ/tCO_2)	5.3	6.3	2.8	3.0	1.8	1.9
	Absorber diameter (m)	2.9	3.0	1.6	1.6	1.2	1.2
	Stripping diameter (m)	2.2	2.4	2.0	2.0	1.8	1.8
[Bmim][acetate]	S-07 IL mass flow (t/h)	122.0	184.6	68.8	84.0	38.7	43.2
	S-07 IL mass purity (%)	100.0	87.5	100.0	87.5	100.0	87.5
	IL conversion (%)	29.0	19.5	49.9	41.1	71.7	62.2
	Regeneration energy (GJ/tCO_2)	4.3	7.0	2.6	3.4	1.6	1.9
	Absorber diameter (m)	2.7	2.9	1.5	1.5	1.0	1.1
	Stripping diameter (m)	1.8	2.3	1.8	2.0	1.6	1.7

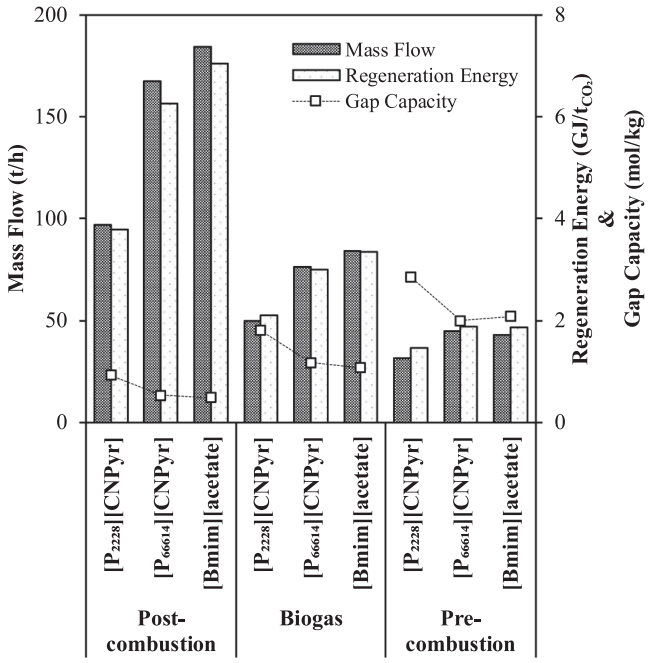

Fig. 12. Correlation between the process gap capacity, mass flow and energy requirements for AHA-ILs and [Bmim][acetate] in post-combustion, biogas and pre-combustion closed processes.

modeled as a packed stripping column using the RADFRAC rigorous model implemented in Aspen Plus, working at 373 K in the reboiler and 0.01 MPa with Rate-based calculations and the reaction module enabled. The energy demand for each IL regeneration depending on the absorption operating conditions is shown in Fig. 9.

As can be observed in Fig. 9, the energy demand in IL regeneration stage drastically decreases at higher CO_2 partial pressure conditions (post-combustion > biogas > pre-combustion system), due to the higher temperatures and lower mass flows (Figs. 3 and 5) of the inlet stream (S-03 in Fig. 1). Regarding the absorbent effect, aa-ILs presents uncompetitive energy requirements upper than 15 GJ/t_{CO2} (post-combustion) compared to the best AHA-IL, $[P_{2228}][CNPyr]$, which needs 3.2 GJ/t_{CO2} in the same conditions and only 1.3 GJ/t_{CO2} after pre-combustion absorption. Most of the energy, > 80%, comes from the reboiler. The analogy between Fig. 9 and the IL demand shown in Fig. 3 proves that the solvent flow rate governs the energy consumption.

In fact, Fig. 10 represents ILs needed mass flow rate in post-combustion configuration and the inlet temperature to the regenerator column. The synergetic effect found in the absorption column plays a major role on improving energy requirements in the regeneration step. Theoretically, a higher enthalpy of reaction should increase the energetic demand in the regeneration, but, in these IL-based cases, the reduction in mass flows and higher temperatures achieved during absorption, fully compensate this drawback, and also reduce further the energy needs on the reboiler.

The stripping column is sized in order to fully describe this unit. Fig. 11 shows the calculated stripping column diameter for the three considered processes depending on the IL employed.

As expected, the stripping column volume decreases at higher CO_2 partial pressures because of the lower inlet flow. Attending to IL selected, [Bmim][acetate] and $[P_{2228}][CNPyr]$ maintain diameters between 1.7 and 2 m for the three CO_2 capture systems and it was slightly increased for [Bmim][i-but] and $[P_{66614}][CNPyr]$ cases. Fig. 11 depicts that aa-ILs need bigger column diameters to regenerate them in comparison to the others ILs studied, particularly attending to the post-combustion process. On the other hand, the difference between operating conditions is not as relevant as in the absorption column because of the lack of CO_2 rich gas flow to be treated and the negligible mass transfer limitations thanks to the elevate operating temperature. Excepting [Bmim][PRO] at post-combustion conditions, all stripping columns respect the industrial range of length to diameter ratio [67].

3.4. Complete processes

After analyzing the CO_2 absorption and IL regeneration operations individually, the complete process was finally closed for the best three resulting ILs ($[P_{2228}][CNPyr]$, $[P_{66614}][CNPyr]$ and [Bmim][acetate]), interconnecting both units and adding on the secondary operations as depicted in Fig. 1. When joining the absorption and the stripping columns, the solvent stream (S-07) that gets into the absorber usually suffers a change in its composition since other compounds are recirculated in minor rates (CO_2-IL product, non-reacted IL, physically absorbed CO_2 and very little traces of N_2, CH_4 or H_2). Table 3 reports the results for the closed processes against the individual units that were previously interpreted in order to study the recirculation effect, in which the S-07 solvent stream is a fresh/neat IL feed.

Regarding the IL needs of the three processes considered, Table 3

Table 4
Process gap capacity *vs.* thermodynamic gap capacity at post-combustion, biogas and pre-combustion CO_2 partial pressures.

Ionic Liquid	Post-combustion		Biogas		Pre-combustion	
	Process Gap Capacity (mol/kg)	Thermodynamic Gap Capacity (mol/kg)	Process Gap Capacity (mol/kg)	Thermodynamic Gap Capacity (mol/kg)	Process Gap Capacity (mol/kg)	Thermodynamic Gap Capacity (mol/kg)
$[P_{2228}]$ [CNPyr]	0.94	1.92	1.82	2.62	2.88	3.31
$[P_{66614}]$ [CNPyr]	0.54	0.83	1.18	1.41	2.01	2.08
[Bmim] [acetate]	0.49	0.67	1.09	1.42	2.11	2.68

shows slightly higher IL request when closing the process, particulary for the post-combustion CO_2 capture, because of not only the lower CO_2 solubility, but also the lower IL conversion as CO_2-IL reaction products are recirculated. Thus, the main effect that recirculated components generate in the absorption operation is slightly increasing the solvent demand. $[P_{2228}]$[CNPyr] gets minimum solvent requirement for all the processes (97 t/h for post-combustion, 50 t/h for biogas and 32 t/h for pre-combustion) and less amount of $[P_{66614}]$[CNPyr] is consumed for post-combustion CO_2 capture (168 t/h) and biogas upgrading (76 t/h) compared to [Bmim][acetate] (185 t/h and 84 t/h, respectively). The calculated absorbent flow needs are remarkably lower than those reported for IL physical solvents using larger columns [22,23] and there is no loss of solvent as is the case, when using conventional amines aqueous solutions.

Concerning the energy balance, Table 3 indicates that regeneration energy required to recover 3.96 t/h of CO_2 with mass purity > 99% suffers a minor increase for AHA-based ILs, but more appreciable for [Bmim][acetate] in the complete process, due to the recirculation effect over the flow rate. Nevertheless, there is no significant differences in the column diameters of closed process results and those of the individual operations. The calculated energy consumptions are in reasonable agreement with those values reported in the literature for $[P_{66614}]$[CNPyr] [65] and [Bmim][acetate] [64], when using simulations that only considered the thermodynamic aspects of the process. $[P_{2228}]$[CNPyr] energy demand is the least. For example, its energy invested for post-combustion CO_2 capture (3.8 GJ/t_{CO2}) is lower compared to other existing technologies for CO_2 capture such as amine-based (4.2 GJ/t_{CO2}) [13] or aqueous ammonia processes (4.1 GJ/t_{CO2}) [59], without involving any energy integration and the mandatory investment cost of the heat-exchanger to carry it out. Moreover, $[P_{2228}]$[CNPyr] is even more promising at higher absorption CO_2 partial pressure conditions. A minimal 1.5 GJ/t_{CO2} was found for pre-combustion capture, close to ILs physical absorbents values at similar working CO_2 partial pressures [22], but much less energy demand than methyl di-ethanol amine (MDEA) in similar processes (3.7 GJ/t_{CO2}) [5].

Rich and lean absorbent loading capacities are frequently reported as their difference, called here process gap capacity, is an useful parameter to explain the absorbent performance in CO_2 capture processes [13,14,59]. It can be calculated as the difference between the CO_2 loading at the absorber inlet (S-07 stream in Fig. 1) and outlet (S-03 stream in Fig. 1) as explained before. Fig. 12 presents the clear relationship between the process gap capacity, mass flow and energy requirements for AHA-ILs and [Bmim][acetate] in post-combustion, biogas and pre-combustion CO_2 capture complete processes. Higher process gap capacity at the CO_2 capture operating conditions implies both lower absorbent and consequently, energy demands.

As can be seen in Fig. 12, $[P_{66614}]$[CNPyr] has 8% superior gap capacity than [Bmim][acetate] for post-combustion treatment (0.54 *vs.* 0.49) and biogas upgrading (1.18 *vs.* 1.09), hence it requires less circulation rate and energy to be regenerated, but at high pressure, [Bmim][acetate] is a more effective alternative for solvent and energy saving due to its greater CO_2 solubility. $[P_{2228}]$[CNPyr] presents the highest gap capacity values in all cases, in agreement with the minimum solvent and energy consumptions obtained for this IL. Table 4 compares the simulated processes gap capacity to the thermodynamic gap capacity, determined through the ILs isotherms at 313 K and 373 K (see Figs. S1 and S3 of Supplementary Material). As can be seen, the thermodynamic gap capacity presents a similar trend to the process gap capacity with independence of the IL type and the CO_2 capture system. Therefore, current analysis concludes that thermodynamic gap capacity can be used to reasonably predict the IL behavior in the complete CO_2 capture process at different operating conditions and, consequently, applied as useful parameter for the adequate selection of IL as CO_2 chemical absorbent.

4. Conclusions

Absorption and desorption operations were simulated for 6 representative ILs in order to evaluate their performance in the complete CO_2 capture processes by chemical absorption using a COSMO-based/Aspen Plus multiscale methodology. Post-combustion, pre-combustion and biogas upgrading operating conditions were analyzed fixing a 90% CO_2 recovery. The results indicate how the solvent flow rate takes a relevant influence on regeneration energy, column sizes and thus it will in the overall CO_2 capture process economics. In this sense, CO_2 solubility, viscosity and enthalpy of reaction were identified as key properties determining the IL performance as CO_2 chemical absorbent. For the studied ILs, major exothermic reactions were proved to both favor the reaction toward product and heat the solvent during the chemical absorption, descending viscosity and allowing CO_2 solubility to control the process over mass transfer kinetics. Therefore, lower solvent flow and regeneration energy are required. Gap capacity is found out to be an adequate parameter to select IL for CO_2 capture by chemical absorption, anticipating the solvent behavior in the complete process. AHA-ILs are consolidated as the most promising ILs-family for CO_2 capture at all the studied CO_2 partial pressures. $[P_{2228}]$[CNPyr] presents the lowest circulation rate and regeneration energy due to its advantageous key properties: moderate viscosity and both highest solubility and heat of reaction. Our results illustrate that IL chemical absorbents can be competitive to current amine-based or aqueous ammonia technologies for post-combustion, biogas and pre-combustion CO_2 capture. Future works should be focused on energy integration and process optimization to perform an economic evaluation.

Declaration of Competing Interest

The authors declare that they have no known competing financial interests or personal relationships that could have appeared to influence the work reported in this paper.

Acknowledgments

The authors are grateful to Ministerio de Economía y Competitividad of Spain (project *CTQ2017-89441-R*) and Comunidad de Madrid (project P2018/EMT4348) for financial support and Centro de Computación Científica de la Universidad Autónoma de Madrid for computational facilities.

Appendix A. Supplementary data

Supplementary data to this article can be found online at https://doi.org/10.1016/j.cej.2020.124509.

References

[1] N. Mac Dowell, P.S. Fennell, N. Shah, G.C. Maitland, The role of CO2 capture and utilization in mitigating climate change, NatureClim. Change 7 (2017) 243.

[2] M. Bui, C.S. Adjiman, A. Bardow, E.J. Anthony, A. Boston, S. Brown, P.S. Fennell, S. Fuss, A. Galindo, L.A. Hackett, J.P. Hallett, H.J. Herzog, G. Jackson, J. Kemper, S. Krevor, G.C. Maitland, M. Matuszewski, I.S. Metcalfe, C. Petit, G. Puxty, J. Reimer, D.M. Reiner, E.S. Rubin, S.A. Scott, N. Shah, B. Smit, J.P.M. Trusler, P. Webley, J. Wilcox, N. Mac Dowell, Carbon capture and storage (CCS): the way forward, Energy Environ. Sci. 11 (2018) 1062–1176.

[3] W.M. Budzianowski, Energy Efficient Solvents for CO2 Capture by Gas-Liquid Absorption: Compounds, Blends and Advanced Solvent Systems, Springer, 2016.

[4] Z. Kapetaki, P. Brandani, S. Brandani, H. Ahn, Process simulation of a dual-stage Selexol process for 95% carbon capture efficiency at an integrated gasification combined cycle power plant, Int. J. Greenhouse Gas Control 39 (2015) 17–26.

[5] A. Padurean, C.-C. Cormos, P.-S. Agachi, Pre-combustion carbon dioxide capture by gas–liquid absorption for Integrated Gasification Combined Cycle power plants, Int. J. Greenhouse Gas Control 7 (2012) 1–11.

[6] M. Asif, M. Suleman, I. Haq, S.A. Jamal, Post-combustion CO2 capture with chemical absorption and hybrid system: current status and challenges, Greenhouse Gases-Sci. Technol. 8 (2018) 998–1031.

[7] P. Luis, Use of monoethanolamine (MEA) for CO 2 capture in a global scenario: consequences and alternatives, Desalination 380 (2016) 93–99.

[8] B. Dutcher, M. Fan, A.G. Russell, Amine-based CO2 capture technology development from the beginning of 2013-a review, ACS Appl. Mater. Interfaces 7 (2015) 2137–2148.

[9] K. Li, W. Leigh, P. Feron, H. Yu, M. Tade, Systematic study of aqueous monoethanolamine (MEA)-based CO2 capture process: Techno-economic assessment of the MEA process and its improvements, Appl. Energy 165 (2016) 648–659.

[10] G. Ferrara, A. Lanzini, P. Leone, M.T. Ho, D.E. Wiley, Exergetic and exergoeconomic analysis of post-combustion CO2 capture using MEA-solvent chemical absorption, Energy 130 (2017) 113–128.

[11] O.W. Awe, Y. Zhao, A. Nzihou, D.P. Minh, N. Lyczko, A Review of Biogas Utilisation, Purification and Upgrading Technologies, Waste and Biomass Valorization, 8 (2017) pp. 267–283.

[12] M.T. Mota-Martinez, J.P. Hallett, N. Mac Dowell, Solvent selection and design for CO2 capture - how we might have been missing the point, Sustainable, Energy Fuels 1 (2017) 2078–2090.

[13] B. Xue, Y. Yu, J. Chen, X. Luo, M. Wang, A comparative study of MEA and DEA for post-combustion CO2 capture with different process configurations, Int. J. Coal Sci. Technol. 4 (2017) 15–24.

[14] E. Oko, B. Zacchello, M. Wang, A. Fethi, Process analysis and economic evaluation of mixed aqueous ionic liquid and monoethanolamine (MEA) solvent for CO2 capture from a coke oven plant, Greenhouse Gases-Sci. Technol. 8 (2018) 686–700.

[15] M. Aghaie, N. Rezaei, S. Zendehboudi, A systematic review on CO2 capture with ionic liquids: current status and future prospects, Renew. Sustain. Energy Rev. 96 (2018) 502–525.

[16] X. Zhang, X. Zhang, H. Dong, Z. Zhao, S. Zhang, Y. Huang, Carbon capture with ionic liquids: overview and progress, Energy Environ. Sci. 5 (2012) 6668–6681.

[17] K. Anderson, M.P. Atkins, J. Estager, Y. Kuah, S. Ng, A.A. Oliferenko, N.V. Plechkova, A.V. Puga, K.R. Seddon, D.F. Wassell, Carbon dioxide uptake from natural gas by binary ionic liquid–water mixtures, Green Chem. 17 (2015) 4340–4354.

[18] S. Sarmad, J.-P. Mikkola, X. Ji, Carbon dioxide capture with ionic liquids and deep eutectic solvents: a new generation of sorbents, ChemSusChem 10 (2017) 324–352.

[19] B. Gurkan, B.F. Goodrich, E.M. Mindrup, L.E. Ficke, M. Massel, S. Seo, T.P. Senftle, H. Wu, M.F. Glaser, J.K. Shah, E.J. Maginn, J.F. Brennecke, W.F. Schneider, Molecular design of high capacity, low viscosity, chemically tunable ionic liquids for CO2 capture, J. Phys. Chem. Lett. 1 (2010) 3494–3499.

[20] M.J. Muldoon, S.N.V.K. Aki, J.L. Anderson, J.K. Dixon, J.F. Brennecke, Improving carbon dioxide solubility in ionic liquids, J. Phys. Chem. B 111 (2007) 9001–9009.

[21] P.J. Carvalho, K.A. Kurnia, J.A.P. Coutinho, Dispelling some myths about the CO2 solubility in ionic liquids, PCCP 18 (2016) 14757–14771.

[22] J. de Riva, J. Suarez-Reyes, D. Moreno, I. Diaz, V. Ferro, J. Palomar, Ionic liquids for post-combustion CO2 capture by physical absorption: Thermodynamic, kinetic and process analysis, Int. J. Greenhouse Gas Control 61 (2017) 61–70.

[23] J. Palomar, M. Larriba, J. Lemus, D. Moreno, R. Santiago, C. Moya, J. de Riva, G. Pedrosa, Demonstrating the key role of kinetics over thermodynamics in the selection of ionic liquids for CO2 physical absorption, Sep. Purif. Technol. 213 (2019) 578–586.

[24] R. Santiago, J. Lemus, D. Moreno, C. Moya, M. Larriba, N. Alonso-Morales, M.A. Gilarranz, J.J. Rodriguez, J. Palomar, From kinetics to equilibrium control in CO2 capture columns using Encapsulated Ionic Liquids ENILs, Chem. Eng. J. 348 (2018) 661–668.

[25] L.F. Zubeir, T.M.J. Nijssen, T. Spyriouni, J. Meuldijk, J.-R. Hill, M.C. Kroon, Carbon dioxide solubilities and diffusivities in 1-alkyl-3-methylimidazolium tricyanomethanide ionic liquids: an experimental and modeling study, J. Chem. Eng. Data 61 (2016) 4281–4295.

[26] L.F. Zubeir, G.E. Romanos, W.M.A. Weggemans, B. Iliev, T.J.S. Schubert, M.C. Kroon, Solubility and diffusivity of CO2 in the ionic liquid 1-butyl-3-methylimidazolium tricyanomethanide within a large pressure range 0.01 MPa to 10 MPa, J. Chem. Eng. Data 60 (2015) 1544–1562.

[27] H. Kolding, R. Fehrmann, A. Riisager, CO2 Capture technologies: current status and new directions using supported ionic liquid phase (SILP) absorbers, Sci. China Chem. 55 (2012) 1648–1656.

[28] J. Lemus, F.A. Da Silva, J. Palomar, P.J. Carvalho, J.A.P. Coutinho, Solubility of carbon dioxide in encapsulated ionic liquids, Sep. Purif. Technol. 196 (2018) 41–46.

[29] G. Cui, J. Wang, S. Zhang, Active chemisorption sites in functionalized ionic liquids for carbon capture, Chem. Soc. Rev. 45 (2016) 4307–4339.

[30] Q.R. Sheridan, W.F. Schneider, E.J. Maginn, Role of molecular modeling in the development of CO2-reactive ionic liquids, Chem. Rev. 118 (2018) 5242–5260.

[31] Z.-Z. Yang, Y.-N. Zhao, L.-N. He, CO2 chemistry: task-specific ionic liquids for CO2 capture/activation and subsequent conversion, RSC Adv. 1 (2011) 545–567.

[32] B.E. Gurkan, T.R. Gohndrone, M.J. McCready, J.F. Brennecke, Reaction kinetics of CO2 absorption in to phosphonium based anion-functionalized ionic liquids, PCCP 15 (2013) 7796–7811.

[33] M.B. Shiflett, D.J. Kasprzak, C.P. Junk, A. Yokozeki, Phase behavior of carbon dioxide + [bmim][Ac] mixtures, J. Chem. Thermodyn. 40 (2008) 25–31.

[34] G. Gurau, H. Rodríguez, S.P. Kelley, P. Janiczek, R.S. Kalb, R.D. Rogers, Demonstration of chemisorption of carbon dioxide in 1,3-dialkylimidazolium acetate ionic liquids, Angew. Chem. Int. Ed. 50 (2011) 12024–12026.

[35] S. Stevanovic, A. Podgorsek, L. Moura, C.C. Santini, A.A.H. Padua, M.F. Costa Gomes, Absorption of carbon dioxide by ionic liquids with carboxylate anions, Int. J. Greenhouse Gas Control 17 (2013) 78–88.

[36] M. Besnard, M.I. Cabaço, F. Vaca Chávez, N. Pinaud, P.J. Sebastião, J.A.P. Coutinho, J. Mascetti, Y. Danten, CO2 in 1-butyl-3-methylimidazolium acetate. 2. NMR investigation of chemical reactions, J. Phys. Chem. A 116 (2012) 4890–4901.

[37] Q. Tian, R. Li, H. Sun, Z. Xue, T. Mu, Theoretical and experimental study on the interaction between 1-butyl-3-methylimidazolium acetate and CO2, J. Mol. Liq. 208 (2015) 259–268.

[38] M.I. Cabaço, M. Besnard, Y. Danten, J.A.P. Coutinho, Carbon dioxide in 1-Butyl-3-methylimidazolium acetate. I. unusual solubility investigated by raman spectroscopy and DFT calculations, J. Phys. Chem. A 116 (2012) 1605–1620.

[39] M.B. Shiflett, B.A. Elliott, S.R. Lustig, S. Sabesan, M.S. Kelkar, A. Yokozeki, Phase behavior of CO2 in room-temperature ionic liquid 1-ethyl-3-ethylimidazolium acetate, ChemPhysChem 13 (2012) 1806–1817.

[40] M.L. Williams, S.P. Holahan, M.E. McCorkill, J.S. Dickmann, E. Kiran, Thermal and spectral characterization and stability of mixtures of ionic liquids [EMIM]Ac and [BMIM]Ac with ethanol, methanol, and water at ambient conditions and at elevated temperatures and pressures, Thermochim. Acta 669 (2018) 126–139.

[41] H.F.D. Almeida, H. Passos, J.A. Lopes-da-Silva, A.M. Fernandes, M.G. Freire, J.A.P. Coutinho, Thermophysical properties of five acetate-based ionic liquids, J. Chem. Eng. Data 57 (2012) 3005–3013.

[42] S. Stevanovic, A. Podgoršek, A.A.H. Pádua, M.F. Costa Gomes, Effect of water on the carbon dioxide absorption by 1-Alkyl-3-methylimidazolium acetate ionic liquids, J. Phys. Chem. B 116 (2012) 14416–14425.

[43] J. Blath, N. Deubler, T. Hirth, T. Schiestel, Chemisorption of carbon dioxide in imidazolium based ionic liquids with carboxylic anions, Chem. Eng. J. 181–182 (2012) 152–158.

[44] C. Moya, N. Alonso-Morales, M.A. Gilarranz, J.J. Rodriguez, J. Palomar, Encapsulated ionic liquids for CO2 capture: using 1-Butyl-methylimidazolium acetate for quick and reversible CO2 chemical absorption, ChemPhysChem 17 (2016) 3891–3899.

[45] R. Santiago, J. Lemus, D. Hospital-Benito, C. Moya, J. Bedia, N. Alonso-Morales, J.J. Rodriguez, J. Palomar, CO2 capture by supported ionic liquid phase: highlighting the role of the particle size, ACS Sustain. Chem. Eng. (2019).

[46] D. Hospital-Benito, J. Lemus, R. Santiago, J. Palomar, Thermodynamic and kinetic evaluation of ionic liquids + tetraglyme mixtures on CO2 capture, J. CO2 Util. (2019).

[47] F.F. Chen, K. Huang, Y. Zhou, Z.Q. Tian, X. Zhu, D.J. Tao, D.E. Jiang, S. Dai, Multimolar absorption of CO2 by the activation of carboxylate groups in amino acid ionic liquids, Angew. Chem. 55 (2016) 7166–7170.

[48] V. Hiremath, A.H. Jadhav, H. Lee, S. Kwon, J.G. Seo, Highly reversible CO2 capture using amino acid functionalized ionic liquids immobilized on mesoporous silica, Chem. Eng. J. 287 (2016) 602–617.

[49] Y.S. Sistla, A. Khanna, CO2 absorption studies in amino acid-anion based ionic liquids, Chem. Eng. J. 273 (2015) 268–276.

[50] R. Santiago, J. Lemus, C. Moya, D. Moreno, N. Alonso-Morales, J. Palomar, Encapsulated ionic liquids to enable the practical application of amino acid-based ionic liquids in CO2 capture, ACS Sustain. Chem. Eng. 6 (2018) 14178–14187.

[51] B. Hong, L.D. Simoni, J.E. Bennett, J.F. Brennecke, M.A. Stadtherr, Simultaneous process and material design for aprotic N-heterocyclic anion ionic liquids in post-combustion CO2 capture, Ind. Eng. Chem. Res. 55 (2016) 8432–8449.

[52] S. Seo, M. Quiroz-Guzman, M.A. DeSilva, T.B. Lee, Y. Huang, B.F. Goodrich, W.F. Schneider, J.F. Brennecke, Chemically tunable ionic liquids with aprotic heterocyclic anion (AHA) for CO2 capture, J. Phys. Chem. B 118 (2014) 5740–5751.

[53] S. Seo, M.A. DeSilva, H. Xia, J.F. Brennecke, Effect of cation on physical properties and CO2 solubility for phosphonium-based ionic liquids with 2-cyanopyrrolide anions, J. Phys. Chem. B 119 (2015) 11807–11814.

[54] L. Sun, O. Morales-Collazo, H. Xia, J.F. Brennecke, Effect of structure on transport properties (viscosity, ionic conductivity, and self-diffusion coefficient) of aprotic heterocyclic anion (AHA) room temperature ionic liquids. 2. Variation of alkyl chain length in the phosphonium cation, J. Phys. Chem. B 120 (2016) 5767–5776.

[55] J. Wu, B. Lv, X. Wu, Z. Zhou, G. Jing, Aprotic heterocyclic anion-based dual-functionalized ionic liquid solutions for efficient CO2 uptake: quantum chemistry calculation and experimental research, ACS Sustain. Chem. Eng. 7 (2019) 7312–7323.
[56] C. Moya, N. Alonso-Morales, J. de Riva, O. Morales-Collazo, J.F. Brennecke, J. Palomar, Encapsulation of Ionic liquids with an aprotic heterocyclic anion (AHA-IL) for CO2 capture: preserving the favorable thermodynamics and enhancing the kinetics of absorption, J. Phys. Chem. B 122 (2018) 2616–2626.
[57] J. de Riva, V. Ferro, C. Moya, M.A. Stadtherr, J.F. Brennecke, J. Palomar, Aspen Plus supported analysis of the post-combustion CO2 capture by chemical absorption using the P-2228 CNPyr and P-66614 CNPyr AHA Ionic Liquids, Int. J. Greenhouse Gas Control 78 (2018) 94–102.
[58] J.J. Fillion, J.E. Bennett, J.F. Brennecke, The viscosity and density of ionic liquid + tetraglyme mixtures and the effect of tetraglyme on CO2 solubility, J. Chem. Eng. Data 62 (2017) 608–622.
[59] J. Yu, S. Wang, Modeling analysis of energy requirement in aqueous ammonia based CO2 capture process, Int. J. Greenhouse Gas Control 43 (2015) 33–45.
[60] M.T. Mota-Martinez, P. Brandl, J.P. Hallett, N. Mac Dowell, Challenges and for the utilisation of ionic liquids as solvents for CO2 capture, Mol. Syst. Des. Eng. 3 (2018) 560–571.
[61] T.E. Akinola, E. Oko, M. Wang, Study of CO2 removal in natural gas process using mixture of ionic liquid and MEA through process simulation, Fuel 236 (2019) 135–146.
[62] Y. Ma, J. Gao, Y. Wang, J. Hu, P. Cui, Ionic liquid-based CO2 capture in power plants for low carbon emissions, Int. J. Greenhouse Gas Control 75 (2018) 134–139.
[63] P. Garcia-Gutierrez, J. Jacquemin, C. McCrellis, I. Dimitriou, S.F.R. Taylor, C. Hardacre, R.W.K. Allen, Techno-economic feasibility of selective CO2 capture processes from biogas streams using ionic liquids as physical absorbents, Energy Fuels 30 (2016) 5052–5064.
[64] M.B. Shiflett, D.W. Drew, R.A. Cantini, A. Yokozeki, Carbon dioxide capture using ionic liquid 1-Butyl-3-methylimidazolium acetate, Energy Fuels 24 (2010) 5781–5789.
[65] H. Zhai, E.S. Rubin, Systems analysis of ionic liquids for post-combustion CO2 capture at coal-fired power plants, Energy Procedia 63 (2014) 1321–1328.
[66] V.R. Ferro, C. Moya, D. Moreno, R. Santiago, J. de Riva, G. Pedrosa, M. Larriba, I. Diaz, J. Palomar, Enterprise ionic liquids database (ILUAM) for use in aspen ONE programs suite with COSMO-based property methods, Ind. Eng. Chem. Res. 57 (2018) 980–989.
[67] G.D. Ulrich, P.T. Vasudevan, Chemical Engineering Process Design and Economics: A, Practical Guide, Process Pub, 2004.